Biochimica et Biophysica Acta 1833 (2013) 1562–1571

Contents lists available at SciVerse ScienceDirect

Biochimica et Biophysica Acta

journal homepage: www.elsevier.com/locate/bbamcr

Expression and processing of fluorescent fusion proteins of amyloid precursor protein (APP)☆

Kathleen Coughlan [a,b,1], Xiangping Huang [a], Xiangyuan He [a,2], Charlotte H.Y. Chung [a,c,3], Guangpu Li [b], Jordan Tang [a,b,c,*]

[a] Protein Studies Program, Oklahoma Medical Research Foundation, Oklahoma City, OK 73104, USA
[b] Department of Biochemistry and Molecular Biology, University of Oklahoma Health Sciences Center, Oklahoma City, Oklahoma 73104, USA
[c] Oklahoma Center for Neuroscience, University of Oklahoma Health Sciences Center, Oklahoma City, OK 73104, USA

ARTICLE INFO

Article history:
Received 4 January 2013
Received in revised form 28 February 2013
Accepted 4 March 2013
Available online 19 March 2013

Keywords:
Amyloid precursor protein
Amyloid-beta
Green fluorescence protein
Beta-secretase
Gamma-secretase

ABSTRACT

Processing of β-amyloid precursor protein (APP) by β- and γ-secretases in neurons produces amyloid-β (Aβ), whose excess accumulation leads to Alzheimer's disease (AD). Knowledge on subcellular trafficking pathways of APP and its fragments is important for the understanding of AD pathogenesis. We designed fusion proteins comprising a C-terminal fragment of APP (app) and fluorescent proteins GFP (G) and DsRed (D) to permit the tracking of the fusion proteins and fragments in cells. CAD cells expressing these proteins emitted colocalized green and red fluorescence and produce ectodomains, sGapp and sRapp, and Aβ, whose level was reduced by inhibitors of β- and γ-secretases. The presence of GappR in endosomes was observed via colocalization with Rab5. These observations indicated that the fusion proteins were membrane inserted, transported in vesicles and proteolytically processed by the same mechanism for APP. By attenuating fusion protein synthesis with cycloheximide, individual fluorescent colors from the C-terminus of the fusion proteins appeared in the cytosol which was strongly suppressed by β-secretase inhibitor, suggesting that the ectodomains exit the cell rapidly ($t_{1/2}$ about 20 min) while the C-terminal fragments were retained longer in cells. In live cells, we observed the fluorescence of the ectodomains located between parental fusion proteins and plasma membrane, suggesting that these ectodomain positions are part of their secretion pathway. Our results indicate that the native ectodomain does not play a decisive role for the key features of APP trafficking and processing and the new fusion proteins may lead to novel insights in intracellular activities of APP.

© 2013 Elsevier B.V. All rights reserved.

1. Introduction

Current evidence supports the idea that excess level of brain amyloid-β peptide (Aβ) is the primary driving force in the pathogenesis of Alzheimer's disease (AD) [1,2]. Hence studying those factors involved in regulating Aβ production is pivotal for understanding the development and treatment of the disease. Aβ, mainly peptides of 40 or 42 amino acids, is generated from the sequential proteolytic cleavage of a membrane protein, β-amyloid precursor protein (APP), by two membrane proteases, β-secretase (memapsin 2, BACE1) and γ-secretase. Within the normal brain, Aβ production and clearance are strictly regulated for fine tuning synaptic function and homeostasis [3]. However, mutations in APP that result in an over production of Aβ, such as the Swedish mutation of APP [4,5] or mutations in γ-secretase that disrupt the Aβ40:Aβ42 ratio, lead to the development of the inherited form of AD [6,7]. Such genetic linkages suggest the importance of maintaining Aβ homeostasis in normal brain functions. The fact that two established risk factors for sporadic AD, ApoE4 [8,9] and SorLA [10] function in cellular trafficking of APP further illustrated the importance of vesicular transport of APP in Aβ homeostasis and AD pathogenesis.

APP is a single chain type I transmembrane glycoprotein with a large ectodomain that contains several subdomains, such as the cupric ion binding domain and the Kunitz type protease inhibitor domain. The processing of APP by β-secretase, at a site located 29 residues from the transmembrane domain, produces the ectodomain fragment, commonly referred as soluble APP (sAPP), and a C-terminal fragment (C99) that consisted of both the transmembrane and the intracellular domains. Processing of APP C99 fragment by γ-secretase at a site within

Abbreviations: APP106, truncated last 106 amino acids of APP; GappR, GFP-APP106-DsRed; RappG, DsRed-APP106-GFP; sGapp, soluble GFP-APP; sRapp, soluble DsRed-APP; sGappα, soluble GFP-APP alpha; sGappβ, soluble GFP-APP beta

☆ This work was supported in part by NIH grant AG18933 to JT.

* Corresponding author at: Protein Studies Program, Oklahoma Medical Research Foundation, Oklahoma City, Oklahoma 73104, USA. Tel.: +1 405 271 7291.
E-mail addresses: Kathleen-coughlan@ouhsc.edu (K. Coughlan), Sean.he@pioneer.com (X. He), Jordan-tang@omrf.org (J. Tang).
[1] Present address: Department of Medicine/Molecular Medicine, 941 Stanton L. Young Blvd. BSEB 312, University of Oklahoma Health Sciences Center, Oklahoma City, OK 73104, USA.
[2] Present address: DuPont Pioneer, 7300 NW 62nd Ave., PO Box 1004, Johnston, IA, USA 50131-0184.
[3] Present address: Center for Neurodegenerative Disease Research, University of Pennsylvania, 3600 Spruce Street 3rd Floor Maloney Building, Philadelphia, PA 19104, USA.

0167-4889/$ – see front matter © 2013 Elsevier B.V. All rights reserved.
http://dx.doi.org/10.1016/j.bbamcr.2013.03.003

the transmembrane domain generates Aβ and the fragment of APP intracellular domain (AICD). γ-Secretase is ubiquitously present in the membranes of all cellular compartments and efficiently cleaves newly generated C99 in the cells (Fig. 1A). Thus, an important step in the regulation of Aβ production is the transport and localization of APP and β-secretase at subcellular compartments where optimal cleavage may take place. Evidence has shown that Aβ production is highly dependent on the cellular trafficking patterns of both APP and β-secretase [11–13]. These proteins are synthesized in the ER, post-translationally modified in the Golgi and transported to the cell surface where APP may be cleaved by α-secretase thereby excluding the formation of Aβ [14]. Alternatively, APP may be internalized with β-secretase into the endosomal system where the acidic interior of the vesicles optimally facilitates β-secretase activity, resulting in APP cleavage leading to Aβ generation [11,15]. After the full process, APP fragments sAPP and Aβ are transported outside of the cells by unknown mechanisms. Among all these steps, the endocytosis of APP appears to be a particularly important process in the regulation of Aβ production.

Several regulatory mechanisms involving the internalization of APP have been reported. Like other type 1 membrane proteins, APP contains sequence motifs in its cytosolic domain that bind various adaptor proteins. Such interactions not only play a pivotal role in packaging APP in transport vesicles for internalization and cellular trafficking, but they also provide sites for regulation of these processes [16,17]. APP is also phosphorylated at several cytoplasmic sites, most notably Thr743 (APP770 numbering), which results in alterations in binding FE65, an important modulator of APP processing and the physiological function of the AICD [17,18]. In addition, most cellular APP is found in the Golgi network, suggesting the presence of a Golgi retention mechanism which may participate in regulating the release of APP to the cell surface.

Current understanding on the trafficking of APP and its fragments in cells is still incomplete. Not only the structural requirements of APP for its trafficking and processing are poorly understood, but also the intracellular pathways for the trafficking of APP fragments are largely obscure. Commonly used methods to study these topics are frequently based on immunohistological staining, which have limited sensitivity and are also ineffective for studying living cells. Previously, Kaether and Gerdes developed a GFP-tagged APP C100-based construct to study the cellular site for γ-secretase cleavage [19]. While informative, this construct had only limited ability in accessing the locale and kinetics of β-secretase cleavage. Furthermore as the label was placed only on the C-terminus of the APP fragment, the visualization of soluble APP was not feasible. To overcome these deficiencies, we sought to create APP constructs that contain intrinsic fluorophores at both termini. Importantly, these modifications should not interfere with the normal processing of APP through the amyloidogenic and non-amyloidogenic pathways. Such APP derivatives would provide information on the structural requirements for APP trafficking and processing. In this paper, we report the design and characterization of such a system used in the studies of APP transport and processing.

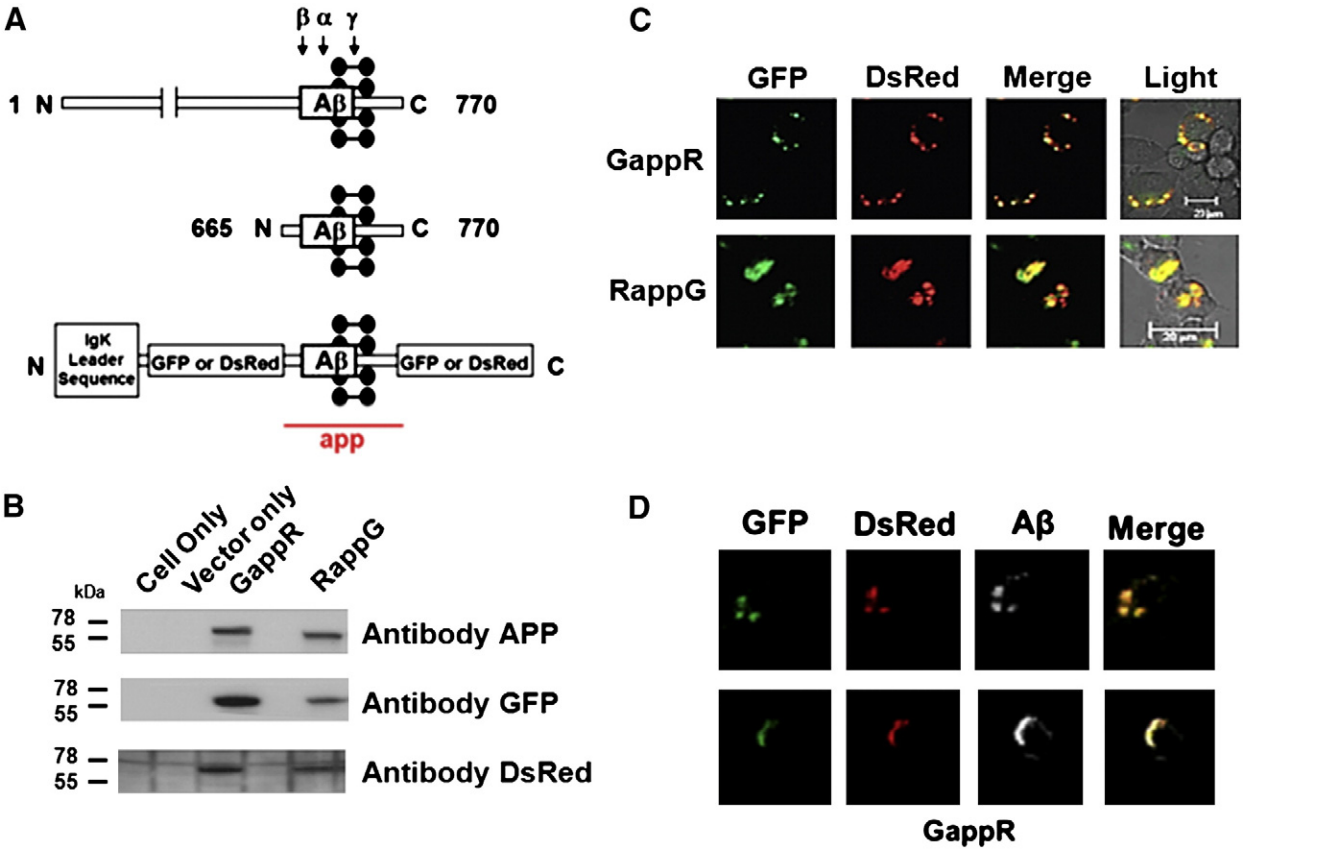

Fig. 1. cDNA construction and expression of GappR and RappG in CNS catecholaminergic CAD cells. A. To generate the GappR or RappG, the last 106 amino acids of APP770 as well as GFP and DsRed were cloned into the pSecTag 2B vector containing an N-terminal IgK leader sequence. The modified app contains amino acids 665–770 including all three secretase sites: β-secretase, α-secretase and γ-secretase (arrows) as well as an intact C-terminal domain and Aβ peptide. B. Immunoblotting of cell lysate following transfection with GappR or RappG for a 24 h period. Antibodies against APP (1560, recognizes Aβ 1-17), GFP and DsRed demonstrated a prominent band between the 55 and 78 kDa markers, which corresponds with the modified apps predicted molecule weight (75 kDa). C. CAD cells were transfected for a 24 h period after which cells were fixed and mounted on slides for visualization using the Zeiss confocal microscope 63× objective. Most cells were positive for both GFP and DsRed fluorescence indicating proper expression of the protein. In addition, the GFP and DsRed fluorescence colocalized with each other suggesting an intact app. D. Under similar conditions as C., GFP and DsRed fluorescence colocalized with APP 1560 suggesting the presence of Aβ. (Scale bar: 20 μm in size).

2. Material and methods

2.1. Construction of modified APPs

The GappR construct contains the last 318 bases of APP which was fused directly with the DsRed cDNA from the pDsRed2-C1 vector (Clontech) to form the appR construct. The appR cDNA was subcloned into a pEGFP-C1 vector (Clontech) thereby generating the GappR. The GappR was subsequently subcloned into a secretion vector, pSecTag 2B (Invitrogen). RappG construction was similar to the GappR except for the reversal in GFP and DsRed fluorophores as well as the use of site directed mutagenesis (Quickchange XL, Stratagene) for correction in alignment of the RappG. Sequence analysis of both GappR and RappG revealed correct sequence and alignment. Tables 1 and 2 found in the supplementary data have the list of primers used for construction of GappR and RappG. Vector for Gapp construct encodes a fusion protein, containing the green fluorescence protein (G) and the last 106 amino acids of APPsw695, inserted in the pSecTag2B vector. The Gapp construct was generated by amplification of the Gapp cDNA from the GappR construct using forward primer 5 ttggatccgtgagcaagggcgagg-3′ and reverse primer 5′-ttctcgagctagttctgcatctgc-3′.

2.2. Cell culture and transfection of GappR or RappG

Mouse neuronal CAD cell line (a gift from Dr. D. M. Chikaraishi, Duke University) was cultured in DMEM/F12 (Fisher) containing 10% fetal bovine serum and 2% penicillin/streptomycin [20]. Transient transfections were performed using Fugene HD (following manufacture's protocol) (Roche) and 2 μg of cDNA for a 12, 24 or 48 h.

2.3. Chemicals, inhibitors and antibodies

GRL-8234 and DAPT (Sigma Aldrich) were separately dissolved in DMSO to concentrations of 12 μM and 1 μM respectively. Cycloheximide was used at a concentration of 100 μg/mL (Sigma-Aldrich). For immunochemical detections, antibodies and dilutions are: GFP (Sigma-Aldrich), 1:4000; DsRed (Clontech), 1:200; APP 1560 (Abcam), 1:2000; actin (Abcam), 1:4000; and phosphor-Thr 743 of APP (Invitrogen), 1:500.

2.4. ELISA

$A\beta_{40}$ was analyzed using a Human $A\beta_{40}$ ELISA kit (Invitrogen) following manufacture's protocol and quantitated in a BioRad 680XR plate reader.

2.5. Western blot

Cells were collected from 6-well plates and lysed in a PBS solution containing 1% NP40, 0.1% SDS, and 1:100 protease inhibitors (Calbiochem). Western blots consisted of steps of PAGE on 10% tricine gel, transferred to a PDVF membrane, and visualized using an ECL kit (Thermo scientific, Pierce).

2.6. Cell viability

Cell viability was determined in a 24 h post transfection of GappR or RappG using the CCK8 counting kit (Dojindo). Trypan blue exclusion was used to assess cell viability after treatment with 100 100 μg/mL cycloheximide for 30 h.

2.7. Subcellular localization

CAD cells were plated on 25 mm glass cover slips (VWR) treated with BD Cell-Tak™ (BD Bioscience). Following transient transfection with GappR or RappG, cells were fixed in 4% paraformaldehyde, mounted on 25 × 75 mm 1.0 mm slides (VWR) using Sure-mount with Dapi (50 μl at 10 mg/mL) and visualized by a Zeiss confocal microscope using the 63× water objective. For co-staining the transfected cells with APP 1560 (1:500) (Abcam), GM130 (Abcam), Lamp2 (Abcam) or EEA1 (Abcam) cells were permeabilized with 0.2% saponin for 15 min at room temperature followed by antibody incubation for 1 h. Secondary antibody, Alexafluor 647 (Invitrogen) goat anti mouse/rabbit was used (1:400) for detection of the above listed antibodies.

2.8. Zeiss confocal microscope fixed cell imaging of processed APP

CAD cells were plated on 25 mm glass cover slips (VWR) treated with BD Cell-Tak™ (BD Bioscience). Following transient transfection with GappR or RappG, and subsequent treatments with cycloheximide, cells were fixed in 4% paraformaldehyde, mounted on 25 × 75 mm 1.0 mm slides (VWR) using Sure-mount with Dapi (50 μl at 10 mg/mL) and visualized by a Zeiss confocal microscope using the 63× water objective.

2.9. Epifluorescent microscope (Zeiss, Axiovert 200M) live cell imaging of processed APP

CAD cells were plated on Willco-Dish glass bottom plated (Willcowells) followed by subsequent treatments. For population studies, snapshots were taken randomly for groups of cells over a 1 h period. Fluorescence was quantitated using the AxioVision software which assessed the average fluorescent intensity in each cell. Subtraction of background fluorescence generated the adjusted fluorescent value. The ratio of C99/sAPPβ (DsRed/GFP) was calculated based on the adjusted values of each fluorophore. A total of 77 cells in two independent experiments were done. For visualization of GappR and RappG cleavage events, cells were randomly chosen based on morphological appearance and images were taken for 3 h every 5 min and fluorescence was quantitated as above which assigned an average fluorescent value to the designated region of interest for each image taken per series. The fluorescent intensities of both GFP and DsRed were assigned and the ratio of each at the given time point was calculated. We averaged three experimental points for each condition and plotted the fluorescent ratio (sAPPβ/C99) over a 3 h time course using 20 min time points. All images were captured using the epifluorescent microscope (Zeiss, Axiovert 200M) with CO_2/heated chamber and a 40× objective lens.

2.10. Statistics

Statistical parameters were assessed using a one-way ANOVA or Student's *t*-test. Values below $p < 0.05$ were considered significant.

3. Results

3.1. Construction and expression of cDNAs for GappR and RappG

The new APP derivative was designed to contain a central APP fragment, app, with two different fluorescence proteins, GFP (G) and DsRed (R), fused to the two ends to form either GappR or RappG (Fig. 1A). These new fusion proteins will test whether APP trafficking and processing can be monitored in real time thereby generating a useful tool for examining the intracellular activities of APP. An important question we sought to answer is if the fused fluorescent proteins are folded correctly and thus can be followed in cells. The availability of two new proteins with G and R at the inverted positions will serve as confirmation to each other in later studies of their processing and transport. The app segment, which is derived from the C-terminal 106 amino acids of the 770 residue $APP_{Swedish}$ (residues 665–770) (Fig. 1A), contains processing sites by three secretases, the transmembrane domain and the cytosolic tail. The app segment also contains those residues known to be preferred for substrate recognition by β-secretase [21,22]. Thus, the processing of the new fluorogenic

proteins through the amyloidogenic and non-amyloidogenic pathways, the transport of various fragments, and the production of intact Aβ can be followed by their fluorescence.

The cDNA's of GappR or RappG were inserted into the vector pSecTag 2B, which contains an IgK leader sequence upstream of multiple cloning sites (Fig. 1A). The expression of GappR or RappG proteins in CAD cells from the respective vectors was assessed by Western blot analysis using antibodies for DsRed, and GFP. We observed positive bands corresponding to a size of 65 kDa (Fig. 1B), which agreed with the expected size for GappR or RappG. Confocal microscopy images of CAD cells transfected with either GappR or RappG showed green and red fluorescence from the expressed GFP and DsRed moieties, and a substantial colocalization of the two images after merging (Fig. 1C). In addition, fluorescence from GFP and DsRed colocalized with antibody 1560 specific for residues 1–17 of Aβ (Fig. 1D) confirming that the intact GappR contains the Aβ species. Together, these observations indicate the successful expression and folding of new proteins GappR and RappG in CAD cells.

3.2. GappR and RappG undergo normal proteolytic processing and post-translational modification of APP

To ensure that the GappR and RappG proteins are able to properly function in cells like the native APP, we investigated their fragments of proteolytic processing and post-translational modification. CAD cells transiently transfected with GappR or RappG vectors and cultured for 24 h produced $Aβ_{40}$ at a level over 20 folds higher than those in untransfected controls (Fig. 2A). The inclusion of 12 μM GRL-8234, a potent β-secretase inhibitor (βi) [23] or 1 μM DAPT, a γ-secretase inhibitor (γi), in the culture medium of the transfected cells resulted in about 90% inhibition of Aβ production (Fig. 2A), while the inclusion of solvent DMSO without the inhibitors produced no inhibition (Fig. 2A; Supplemental Fig. 1). In addition, we also observed in the Western blot of culture medium a 33 kDa band corresponding to the ectodomain of GappR, sGappβ, which is a direct product of β-secretase cleavage of GappR (Fig. 2B). This band was absent when β-secretase inhibitor GRL-8234 was added to the culture medium (Fig. 2B), confirming that it was the cleavage product of β-secretase. These findings suggest that similar to native APP, GappR and RappG are processed normally by β-secretase and γ-secretase through the amyloidogenic pathway.

In the non-amyloidogenic pathway, APP is cleaved first by α-secretase to generate a secreted sAPPα fragment and a membrane tethered C83 fragment. The latter is further processed by γ-secretase to produce a p3 fragment and the AICD. In Western blots of the culture medium of cells expressing GappR, using antibody 1560 which recognizes only sGappα but not sGappβ, we observed a 35-KDa band corresponding to the predicted size of sAPPα (Fig. 2B). In the presence of β-secretase inhibitor GRL-8234, the intensity of the sAPPα band is increased by about 4 fold compared to those samples containing no inhibitor (Fig. 2B). These comparisons indirectly substantiated the identity of the sAPPα bands as it is well known that the suppression of the amyloidogenic pathway would result in the elevation of APP processing through the non-amyloidogenic pathway mediated by α-secretase [24].

APP contains eight phosphorylation sites on its C-terminal cytosolic tail, one of which, threonine 743 (APP770 numbering) has been shown to be the major phosphorylation site in APP [18]. From Western analyses using a phospho-specific antibody that recognizes the sequence surrounding the phosphate group at Thr743, we found that both GappR and RappG are phosphorylated (Fig. 2C). The above observations indicate that GappR and RappG retain many of the processing and phosphorylation functions of APP in the cells.

3.3. Intracellular localization of GappR

Examined under a confocal microscope, the fluorescence of GappR expression in CAD cells produced punctate, vesicular-like bodies in the perinuclear region (Fig. 3A). These GappR-vesicle like structures did not colocalize with the late endosome/lysosome marker Lamp2 nor the Golgi marker GM130 (Fig. 3B). They also colocalize poorly with endosome marker EEA1 (data not shown). It is known, however, that APP and EEA1 colocalize poorly in some cultured neuronal cells and not at all in other neuronal cell lines [25,26]. To examine the colocalization of GappR with early endosomes in CAD cells, the Rab5 antibody was employed following GappR transfection. At a 6 h post transfection, we observed clear colocalization of the two proteins (Fig. 3C). Interestingly, less extent of colocalization was found in expression periods of 12 h or longer. This appeared to be due to the disparity between the high fluorescence intensity from GappR and relatively weak fluorescence intensity from Rab5. The above observations are consistent with the intracellular localization of GappR in endosomes.

3.4. Visualization of GappR and RappG processing through confocal microscopy

GappR expressed in CAD cells and its proteolytic products should be distinguishable when examined with confocal microscopy. While GappR is expected to have colocalized GFP and DsRed fluorescence, the proteolytic fragments alone should produce images of a single fluorophore. We observed initially intense colocalized green and red fluorescence within most cytosolic areas in the cells but only a few small areas of single fluorescence (Fig. 3A). In order to increase the chance for observing the fragments, we attempted to shift the synthetic/degradation dynamics using protein synthesis inhibitor cycloheximide (CHX), which had been successfully employed for this purpose previously [27]. We investigated CHX dosage as related to the inhibition of GappR synthesis (Supplementary Fig. 2) which provided a range of workable conditions for further experiments. Confocal microscopic images of GappR expressed in the presence of CHX showed clear green or red vesicular-like areas in the cytosolic region at the 6 h and 12 h time points (Fig. 4A). These observations suggest that the attenuated protein synthesis with CHX improved the observation of GappR cleavage products sGappβ (green vesicles) and C99R (red vesicles).

To ensure that CHX addition did not alter the mechanism of APP processing, we set out to detect Aβ in those cells treated with CHX (Fig. 4B). Cells were transfected with GappR and cultured for 12 h in the presence or absence of β-secretase inhibitor GRL-8234 or γ-secretase inhibitor DAPT. After which, CHX was added for 6 h, and the media collected for the determination of Aβ. As expected, CHX reduced Aβ by about 40% as compared to control (Fig. 4B). Combination of CHX with secretase inhibitors further reduced Aβ, indicating that a substantial capacity of APP processing was still functioning in the presence of CHX. In another series of experiments, culture media from cells treated as described above were replaced with CHX free media or media with the inhibitor additives and Aβ accumulated over the next 25 h was measured. Cells which had been treated with CHX produced only about 10% of Aβ as compared with the CHX free control (Fig. 4B). This difference is expected as CHX had inhibited the synthesis and accumulation of GappR in the previous period. Significantly, secretase inhibitors further inhibited Aβ level in the CHX treated cells. These observations suggest that the APP processing apparatus in the cells was functional during or after CHX treatment, thus, it would be possible to follow the localization, processing and transport of GappR in CHX treated cells.

3.5. Visualization of GappR and RappG processing through the use of live cell imaging

The results presented above suggest that using the developed GappR and RappG expression system, the dynamic processes of APP cleavage and transport may now be followed in live cells using the epifluorescent microscope (Zeiss, Axiovert 200M) with environmental chamber. Our initial attempt was aimed at capturing cellular images of green or red fluorescence which provide visual markers for the processing of

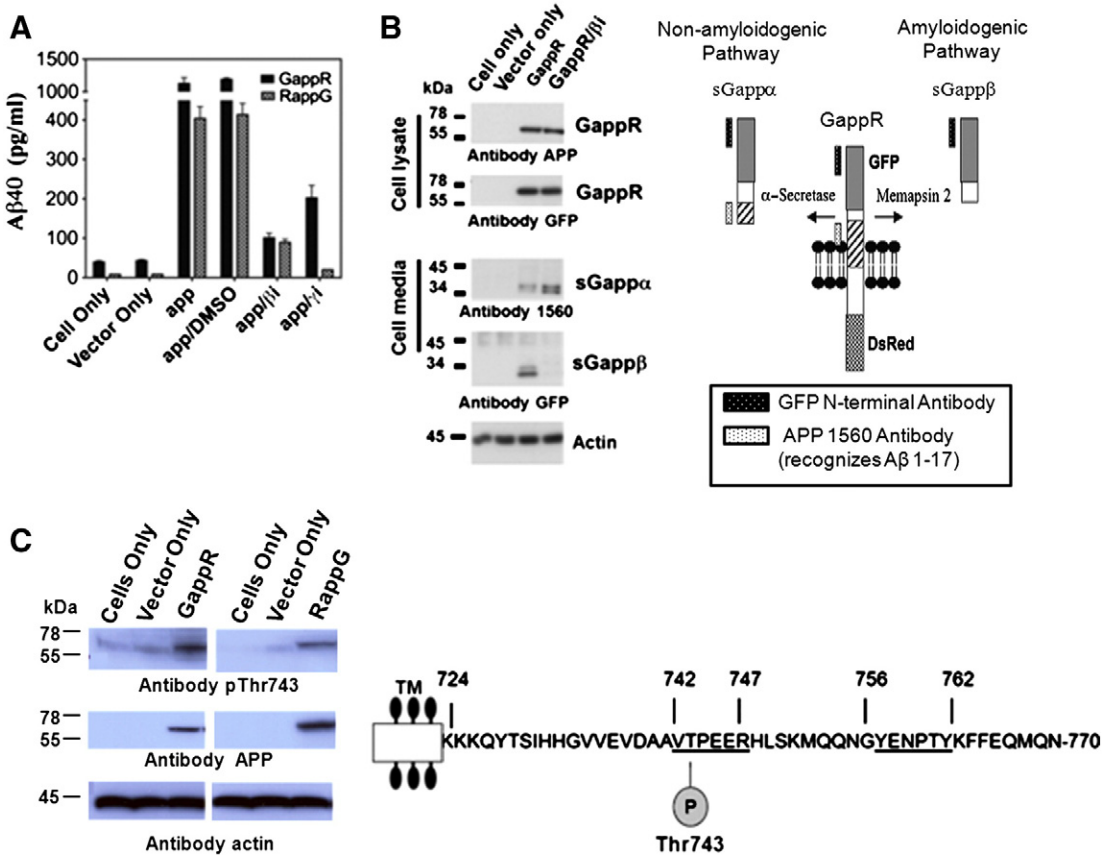

Fig. 2. GappR and RappG are processed through the amyloidogenic and non-amyloidogenic pathways as well as undergo post-translational modification on Thr 743. A. CAD cells transfected with GappR or RappG for a 24 h period had detectable levels of Aβ production in the cell media. Further confirmation of this came from the use of a β-secretase inhibitor GRL-8234 (βi) and γ-secretase inhibitor DAPT (γi). Both inhibitors halt the amyloidogenic pathway thereby reducing the production of Aβ. B. Schematic showing the specific epitopes for GFP and APP 1560 antibodies. In terms of the sGapps, GFP is able to recognize both sGappα and sGappβ, however, APP 1560 will only recognize sGappα. Immunoblotting for cell lysate and media after a 48 h transfection with GappR. Using antibodies APP 1560 and GFP on cell lysate demonstrated that GappR expression is similar despite the addition of GRL-8234. Moreover, the cell media showed a decrease in sAPPβ upon addition of GRL-8234, but an increase in sGappα. Confirmation of sGappα was demonstrated through the use of a specific antibody, APP 1560, that only recognizes this species. Modest amounts of sGappα exist under normal conditions in the cell media, however, upon addition of GRL-8234, an increase in this product is detected due to the inhibition of the amyloidogenic pathway. C. Schematic representing the C-terminal domain of APP. In bold are the two signature motifs VTPEER and YENPTY. The major APP phosphorylation site occurs at Thr743, which is part of the VTPEER motif. Western blot confirmed the ability of GappR and RappG to be phosphorylated at their C-terminal Thr743 site.

GappR/RappG. Fluorescent microscopic images of GappR transfected cells from the merge of green and red fluorescence showed significant intensity of red fluorescence, indicating the presence of C99-DsRed fragment in the cells (Fig. 5A) which substantiated the presence of GappR processing. Conversely, the addition of GRL-8234 resulted in a merged image that was essentially yellow, indicating similar intensities for both the GFP and DsRed fluorophores. The presence of both GFP and DsRed in the cell suggests that the processing of GappR was suppressed by the β-secretase inhibitor (Fig. 5A). The ratio for red and green fluorescence in an individually chosen cell from a non-treated and inhibitor treated condition was calculated (Fig. 5B). Similar calculations were done for all 77 cells in both conditions and plotted on a scatter plot (Fig. 5C). The DsRed to GFP ratio was greater in GappR transfected cells compared to cells with inhibitor ($p < 0.001$). Furthermore, 68% control cells had the red/green ratios greater than 2, this fraction was only 27% in cells with inhibitor ($p < 0.001$) (Fig. 5 D). Since it is known that sAPP is secreted from the cells, the loss of green fluorescence from GappR processing suggests that the sGapp fragment is rapidly removed from the cells, possibly by secretion, and the other fragment C99R is retained.

3.6. Course of GappR and RappG processing observed through live cell imaging

We next attempted to observe the course for the processing of GappR by β-secretase in living cells using the established conditions described above. CAD cells were transiently transfected with GappR and cultured for 12 h in the absence or presence of β-secretase inhibitor GRL-8234, then in the presence of CHX for 16 h. Cells were then observed for GFP and DsRed fluorescence for 3 h in 30 min intervals. We observed a significant and steady decrease in GFP fluorescence in control cells within the first hour but remained the same thereafter (Fig. 6A). In the presence of GRL-8234, there was no significant loss of GFP fluorescence (Fig. 6A), again indicating the loss of GFP fluorescence was mediated by β-secretase. To substantiate these results, we repeated this experiment using cells transfected with RappG and found a loss of DsRed fluorescence in control cells in the initial 60 min which was very similar to that observed for GappR in the experiment above. Again, inhibitor GRL-8234 abolished the DsRed loss (Fig. 6B). These observations were verified with quantitative data on ratios of two fluorescence intensities (Fig. 6C). In the presence of inhibitor GRL-8234, the ratios of fluorescence from GappR and RappG remained near 1:1 throughout the 3 h observation period, indicating that little processing had taken place. In the control experiments, the decline of fluorescence ratios, which reflects the loss of C-terminal C99 moiety, leveled off at about 0.55.

3.7. Visualization of sGapp and sRapp through the use of live cell imaging

When APP is cleaved by β-secretase in the endosomes, the soluble N-terminal ectodomain, sAPPβ, is released from the membrane

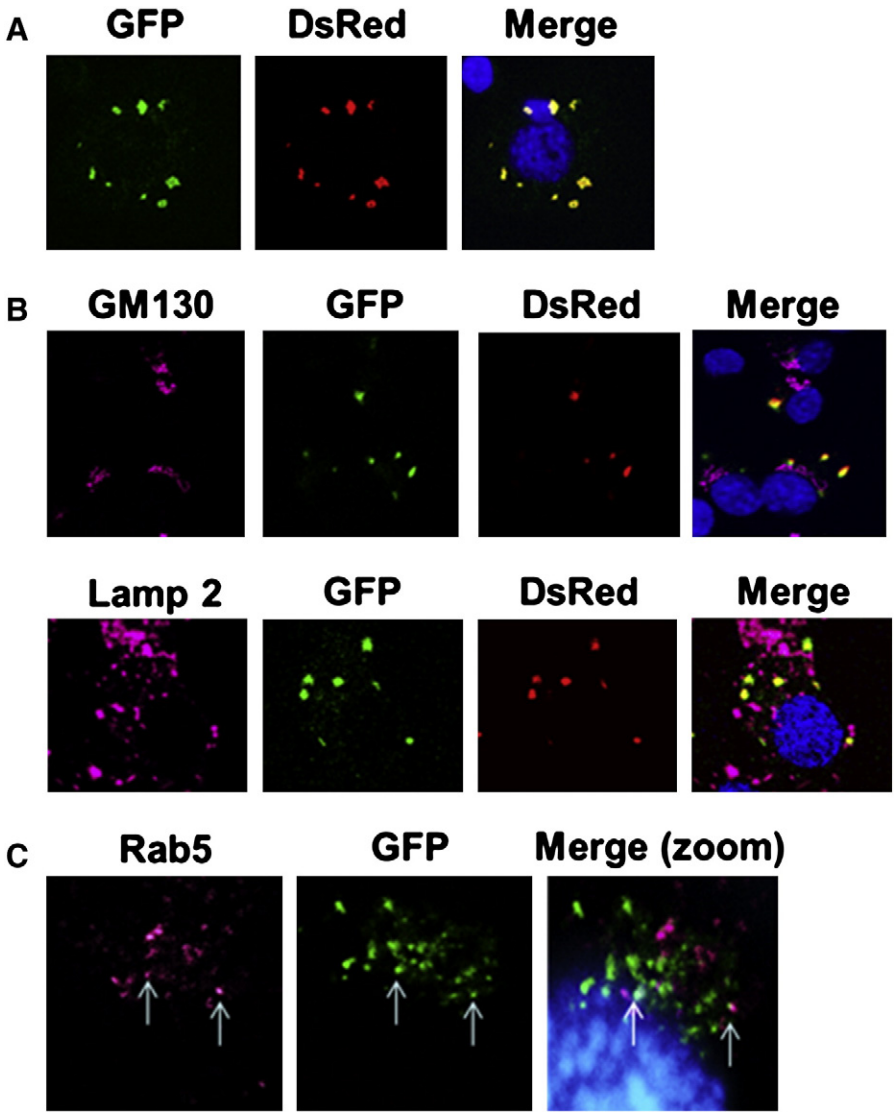

Fig. 3. GappR forms punctate like vesicle structure in the cytoplasm some of which correspond to Rab 5 positive vesicles. A. CAD cells were transfected for a 24 h period after which cells were fixed and mounted on slides for visualization using the Zeiss confocal microscope 63× objective. Most cells expressed punctate like vesicle staining in the cytoplasm. B. Under similar conditions as A., co-staining with GM130 Golgi marker or Lamp2 lysosomal marker revealed very little colocalization with GappR. C. CAD cells transfected for 6 h were co-stained with Rab5 early endosomal marker. Colocalization between GappR and Rab 5 (arrows) indicated localization of GappR in early endosomes.

within the vesicles and transported outside of the cells. The transport system for sAPPβ has not been observed and its mechanism remains obscure. The data presented above indicate that, during the cleavage of GappR or RappG by β-secretase, the N-terminal fragments, sGappβ or sRappβ, which are equivalent to sAPPβ in APP, are rapidly removed from the cell. Therefore, we sought to observe, as a model of sAPPβ, the transport of sGappβ and sRappβ using live cells expressing GappR or RappG. CAD cells were transiently transfected and cultured for 12 h, followed by incubation in the presence of CHX for 2–6 h, then observed under an epifluorescent microscope. We assumed that the subcellular components involved in the transport of these two fragments will emit a single color in a fluorescence microscope, green for sGappβ and red for sRappβ. We observed in some cells patches of vesicle-like structures within the cytosolic region of the cells for both app constructs (Fig. 7A). They were clearly distinguishable from those containing uncleaved GappR or RappG which emitted two fluorescent signals (yellow after merge). Interestingly, these red/green areas were found on one side of the cells adjacent to the large area of unprocessed GappR or RappG (Fig. 7A, yellow merged areas) but bridging toward the plasma membrane (Fig. 7A). Using confocal microscopy, these vesicle-like structures showed poor colocalization with Lamp2, a known marker for late endosomes/lysosomes (Fig. 7B). These results suggest that the red/green areas may be part of a transport system and this secretion activity is polarized in cells.

4. Discussion

Results presented above indicate that in the new APP fusion proteins expressed in CAD cells, the fluorophore moieties, GFP and DsRed, were correctly folded to yield green and red fluorescence respectively. In the subcellular areas where fluorescence from two fluorophores colocalized, the intensities of the two fluorophores were similar suggesting that the fluorophores at the two ends of the new proteins are both functional. Moreover, the successful transit of the fusion proteins through the secretory and endocytic pathways supports the correct folding since the incorrectly folded proteins are known to be retained by the endoplasmic reticulum. Our data also indicated that the fusion proteins were inserted into the membrane with the app moiety recognized by the same cellular mechanisms involved in the transport and processing of native APP. We not only observed the expected GappR and RappG fragments processed by β- and γ-secretases (Figs. 1 and 2), but also the inclusion of specific and potent inhibitors

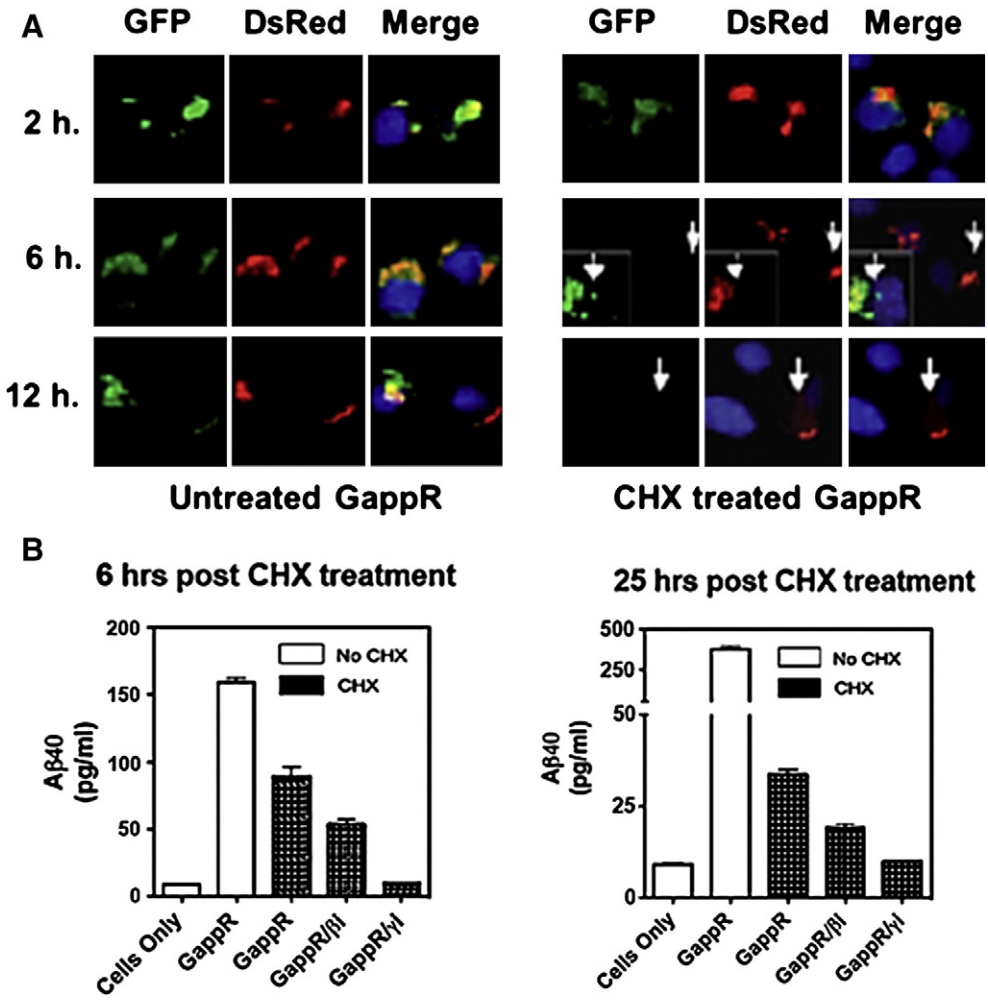

Fig. 4. Addition of CHX enhances detection of sGapp and C99R fragments derived from the processing of GappR. A. CAD cells were transfected for a 24 h period after which cells were untreated or treated with 100 ug/mL of CHX for 2, 6 or 12 h. Cells were fixed and mounted on slides for visualization using the Zeiss confocal microscope 63× objective. Most cells expressed punctate like vesicle staining in the cytoplasm. Treated samples expressed enhanced distinct GFP or DsRed fluorescence indicative of sGapp or C99R respectively. B. CAD cells were transfected for a 12 h period after which cells were untreated or treated with 100 ug/mL of CHX for either 6 h or 26 h in the presence of APP inhibitors GRL-8234 or DAPT. Aβ production was not inhibited with the addition of cycloheximide.

to these proteases that greatly decreased the level of fusion protein fragments as well as Aβ. In addition, the inhibition of β-secretase led to a higher level of processing of the fusion proteins by α-secretase, which is a well known compensatory response in APP processing in cells by these two secretases [17]. The fact that GappR and RappG are phosphorylated at Thr-743 as in native APP also substantiates the correct folding and transport of the fusion proteins. Since APP and its processing secretases are membrane associated proteins, our data suggest that the app moiety of the protein is inserted into the cell membrane with the same topological relationships to these proteases as for the native APP and the fusion proteins are transported to the appropriate subcellular compartments for APP processing. These observations also suggest that the ectodomain does not play a decisive role in the key features of APP trafficking and processing. In addition, the fusion of fluorescent proteins to the C-terminal does not significantly impede the trafficking and processing mechanisms of APP.

Even though the fusion proteins retained the trafficking pathway of APP, some changes in the quantitative subcellular distribution may be anticipated. We saw a clear difference in the level of APP and the fusion proteins in the Golgi. It is well known that under the normal conditions, about 90% of cellular APP is in the Golgi which seems to serve as a reservoir of APP supply to cell surface and endosomes [17]. For GappR and RappG, however, little colocalization was seen for these fusion proteins with Golgi marker GM130 indicating that the GFP or DsRed moiety may affect app retention. Instead, most of the GappR and RappG were found to be located in unidentified punctate like vesicle structures within the cell (3a). Interestingly, a similar construct (Gapp) lacking the C-terminal fluorophore, DsRed, was constructed and functioned similar to native APP. The Gapp produced Aβ and showed strong Golgi retention indicating that the C-terminal tail of APP may play a role in its recognition or release from Golgi (Supplemental Fig. 3). Although the mechanism of this effect is not yet clear, the reduced Golgi retention of the fusion proteins does not seriously impact on the original goal of our study since the intracellular transport pathway of APP to be studied by the new proteins remains intact.

Our initial attempt to follow the processing of the new fusion proteins was to observe the processed fragments by taking advantage of their single green or red fluorescence. However, in CAD cells expressing either GappR or RappG, nearly all of the green and red fluorescent lights were colocalized (Fig. 4) at different time points after transfection (data not shown). Significant cellular areas with single fluorescence corresponding to the C-terminal fragments were seen, however, after the attenuation of protein synthesis with cycloheximide (Fig. 4). The effect of cycloheximide on APP processing and trafficking is predictably multifaceted. In the untreated cells, the level of the unprocessed fusion proteins appears to be in great excess of the processed fragments and the overpowering fluorescence from the fusion protein prevented an

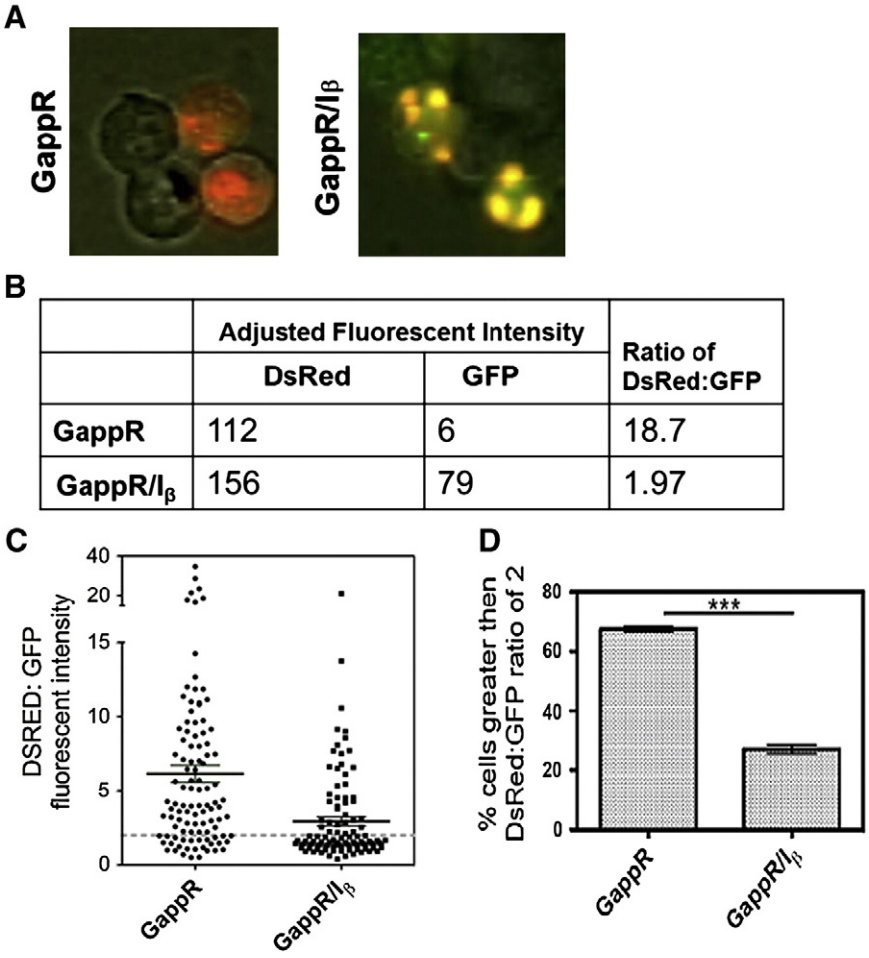

	Adjusted Fluorescent Intensity		Ratio of DsRed:GFP
	DsRed	GFP	
GappR	112	6	18.7
GappR/Iβ	156	79	1.97

Fig. 5. Addition of CHX results in production of C99R in CAD which is inhibited by GRL-8234. A. Representative population of CAD cells transfected in the absence or presence of GRL-8234 for 12 h followed by an additional 18 h with CHX treatment. GappR expressing cells show predominantly red only staining indicating the presence of C99R. Addition of GRL-8234 results in blockage of GappR cleavage by β-secretase, thereby resulting in an accumulation of intact (yellow) protein containing both GFP and DsRed fluorescence. B. Representative calculation (AxioVision software) for the DsRed:GFP ratio used in panel C to plot all 77 samples. C. Quantitation of DsRed:GFP fluorescent ratio in CAD cells under the above conditions using AxioVision software. Those cells expressing GappR show higher levels of DsRed only staining compared to the GRL-8234 treated cells. D. Graph representing the percent of cells greater than a 2 fold increase in the DsRed:GFP ratio. Those cells treated with GRL-8234 had fewer cells that expressed solely DsRed whereas the nontreated cells had an abundant number of cells expressing DsRed only.

effective observation of the processed products. Among many possible effects, cycloheximide should reduce the cellular level of fusion proteins to permit a more clear observation of the C-terminal fragments. Regardless which effects are operative, it is important to point out that the inhibition of protein synthesis may affect the dynamics but not the fundamental mechanism of the processing and transporting systems for the fusion proteins. Thus, the observations made in cycloheximide treated cells can still be a model for APP processing and transport in untreated cells. We saw little change in the intensity of these single fluorescence areas up to 36 h (results not shown). Since the resolution of the fluorescence microscope was not sufficiently high to observe individual secretion vesicles, it is more likely that the observed vesicular fluorescent areas containing C99 represent subcellular regions, such as endosomes, with a relative abundance of this fragment.

The capturing of fluorescent images representing C-terminal fragments is supported by the following observations. While the expression of RappG produced subcellular areas of singular green fluorescence, the expression of GappR produced predominantly red fluorescence, indicating that this fluorescence comes from the fluorophores in the C-terminal C99-containing fragments. The presence of the single red/green areas was suppressed by specific inhibitors for β- or γ-secretases, indicating that these C-terminal fragments were the products of these two secretases through the amyloidogenic pathway. Moreover, the change in the ratio of the two fluorophores in live cells at different times after the removal of β-secretase inhibitor (Fig. 6) is also consistent with the above interpretations. These results suggest that the cellular retention of the N- and C-terminal fragments from β-secretase processing was not the same and the N-terminal fragment, sGapp or sRapp, had a shorter residence time than their C-terminal counterparts. Since sAPP is known to be secreted into the medium, it seems probable that the relatively fast disappearance of sGapp and sRapp from the cells is due to the secretion of these fragments.

Using the combination of an early transfection expression period and a short cycloheximide inhibition, we observed fluorescence corresponding to sGapp and sRapp in live cells (Fig. 7). The identity of these fragments was again verified by the change of red and green fluorescence with the use of two different fusion constructs. It is interesting that these fluorescent areas are mostly located between the fusion protein areas (colocalized green and red, presumably endosomes) and the plasma membrane. We observed that these structures showed little colocalization with the Lamp2, a late endosome/lysosome marker suggesting that the majority of visible sAPP is not accumulating in the degradative pathway. However, these structures do not have the expected properties of the transport vesicles for sAPP. First, they are fairly stationary in their positions as contrast to the highly mobile nature expected of the secretary vesicles. Second, most of these structures are larger in size than expected for transportation vesicles. In addition, these structures have a steady level of fluorescence

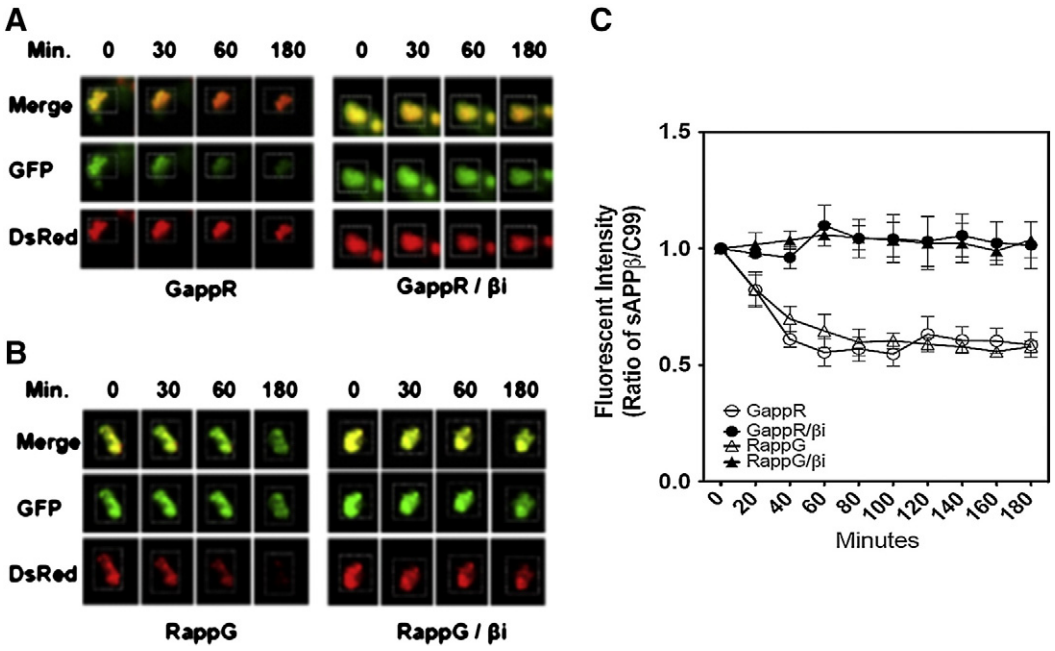

Fig. 6. Live cell imaging of Gapp and Rapp processing in CAD cells. A. Representative population of CAD cells transfected with GappR in the absence or presence of GRL-8234. Live cell imaging over a 3 h period demonstrated a loss of GFP fluorescence in nontreated cells compared to the GRL-8234 treated cells indicating GappR processing. B. Representative population of CAD cells transfected with RappG in the absence or presence of GRL-8234. Live cell imaging over a 3 h period demonstrated a loss of DsRed fluorescence in nontreated cells compared to the GRL-8234 treated cells indicating RappG processing. C. Graphical representation for A and B, representing the ratio of sAPPβ/C99 over a 3 h period. Both GappR and RappG demonstrated equal app processing kinetics with peak reduction occurring at the 60 min time point.

over the time up to 18 h when the endosomes are losing either red or green fluorescence. This suggests that there is a stable steady state of fluorescent content in these structures. A possible explanation for their identity is that they are the 'transfer stations' for the secretion of sAPP. It is well known that the endosomal system contains assemble centers. Thus, it is reasonable that 'transfer stations' may serve to channel the N-terminal fragments to different cellular destinations. The fact that we did not observe the mobile transport vesicles is not surprising since they have been difficult to observe in all phases of intracellular trafficking and the resolution of the live cell microscopy is not expected to have such

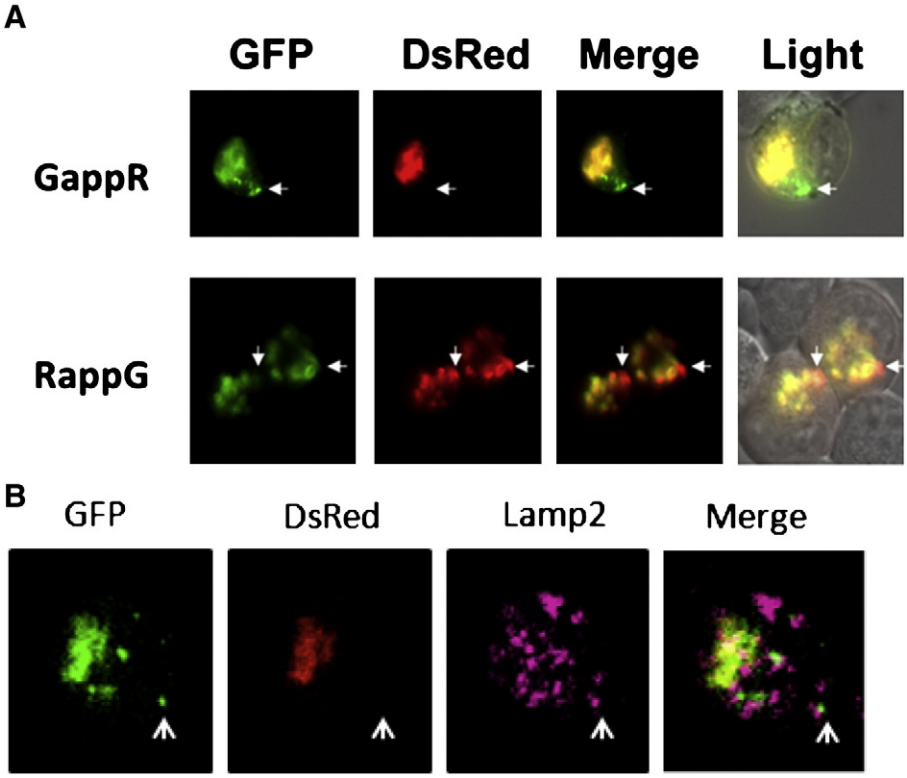

Fig. 7. Visualization of sGapp and sRapp through the use of live cell imaging. A. CAD cells were transfected with GappR or RappG and cultured for 12 h, followed by incubation in the presence of CHX for 2–6 h, then observed under a fluorescence microscope. Punctate green or red only vesicles were pronounced in the cytoplasmic region of these cells demonstrating a polarized accumulation of sGapp and sRapp respectively. B. Similar to A, the polarized accumulation of sGapp shows weak colocalization with Lamp2, a late endosome/lysosome marker.

capability. Despite the unknown identity for these structures, our results demonstrate the potentials of using these fluorescent APP derivatives as tracking device and suggest for the first time a secretion mechanism for sAPP that can be further studied in detail. The usefulness of the former has been further demonstrated in a separate study in which the Golgi residence of APP and Gapp was perturbed by guanidinium compounds (Chung, Cooley, Huang, He and Tang, Abstract of the Neuroscience meeting, 2009, and manuscript submitted for publication). The fluorescence of Gapp was a convenient tool in assessing such cellular redistribution.

5. Conclusions

The endosomal system plays a key role in APP processing and its regulation, intimate to the pathogenesis of Alzheimer's disease, is of great scientific and medical interests. However, a serious problem in studying APP trafficking is the difficulty to accurately and sensitively identify the location of APP while it transits through the secretory pathway, endocytic pathway and processing steps. Classical methods including immunohistological stains with APP antibodies not only lack sensitivity, but they are also inappropriate for detecting APP in living cells. The fusion APP proteins described here may provide a way to overcome these limitations. We have shown that the fluorescence from the fusion proteins and their fragments can be followed in cells, including live cells. The authenticity of the fluorescence sources can be verified through the use of two reversed constructs. With future studies to manipulate cellular conditions and to improve observation resolutions, such constructs will be powerful new tools for studying the mechanism, regulation and kinetics of APP trafficking.

Supplementary data to this article can be found online at http://dx.doi.org/10.1016/j.bbamcr.2013.03.003.

Acknowledgements

The authors thank Dr. Fluoro Lupu, for his insight and scientific advice regarding this project, Ben Fowler and Julie Maier for their assistance with live cell imaging, and Debbie Downs for her technical assistance. J.T. is the holder of the J. G. Puterbaugh Chair in Biomedical Research at the Oklahoma Medical Research Foundation.

References

[1] D.J. Selkoe, The molecular pathology of Alzheimer's disease, Neuron 6 (1991) 487–498.
[2] D.J. Selkoe, Translating cell biology into therapeutic advances in Alzheimer's disease, Nature 399 (1999) A23–A31.
[3] F. Kamenetz, T. Tomita, H. Hsieh, G. Seabrook, D. Borchelt, T. Iwatsubo, S. Sisodia, R. Malinow, APP processing and synaptic function, Neuron 37 (2003) 925–937.
[4] X.D. Cai, T.E. Golde, S.G. Younkin, Release of excess amyloid beta protein from a mutant amyloid beta protein precursor, Science 259 (1993) 514–516.
[5] M. Citron, T. Oltersdorf, C. Haass, L. McConlogue, A.Y. Hung, P. Seubert, C. Vigo-Pelfrey, I. Lieberburg, D.J. Selkoe, Mutation of the beta-amyloid precursor protein in familial Alzheimer's disease increases beta-protein production, Nature 360 (1992) 672–674.
[6] K. Duff, C. Eckman, C. Zehr, X. Yu, C.M. Prada, J. Perez-tur, M. Hutton, L. Buee, Y. Harigaya, D. Yager, D. Morgan, M.N. Gordon, L. Holcomb, L. Refolo, B. Zenk, J. Hardy, S. Younkin, Increased amyloid-beta42(43) in brains of mice expressing mutant presenilin 1, Nature 383 (1996) 710–713.
[7] N. Suzuki, T.T. Cheung, X.D. Cai, A. Odaka, L. Otvos Jr., C. Eckman, T.E. Golde, S.G. Younkin, An increased percentage of long amyloid beta protein secreted by familial amyloid beta protein precursor (beta APP717) mutants, Science 264 (1994) 1336–1340.
[8] E.H. Corder, A.M. Saunders, W.J. Strittmatter, D.E. Schmechel, P.C. Gaskell, G.W. Small, A.D. Roses, J.L. Haines, M.A. Pericak-Vance, Gene dose of apolipoprotein E type 4 allele and the risk of Alzheimer's disease in late onset families, Science 261 (1993) 921–923.
[9] W.J. Strittmatter, A.M. Saunders, D. Schmechel, M. Pericak-Vance, J. Enghild, G.S. Salvesen, A.D. Roses, Apolipoprotein E: high-avidity binding to beta-amyloid and increased frequency of type 4 allele in late-onset familial Alzheimer disease, Proc. Natl. Acad. Sci. U. S. A. 90 (1993) 1977–1981.
[10] E. Rogaeva, Y. Meng, J.H. Lee, Y. Gu, T. Kawarai, F. Zou, T. Katayama, C.T. Baldwin, R. Cheng, H. Hasegawa, F. Chen, N. Shibata, K.L. Lunetta, R. Pardossi-Piquard, C. Bohm, Y. Wakutani, L.A. Cupples, K.T. Cuenco, R.C. Green, L. Pinessi, I. Rainero, S. Sorbi, A. Bruni, R. Duara, R.P. Friedland, R. Inzelberg, W. Hampe, H. Bujo, Y.Q. Song, O.M. Andersen, T.E. Willnow, N. Graff-Radford, R.C. Petersen, D. Dickson, S.D. Der, P.E. Fraser, G. Schmitt-Ulms, S. Younkin, R. Mayeux, L.A. Farrer, P. St George-Hyslop, The neuronal sortilin-related receptor SORL1 is genetically associated with Alzheimer disease, Nat. Genet. 39 (2007) 168–177.
[11] X.P. Huang, W.P. Chang, G. Koelsch, R.T. Turner III, F. Lupu, J. Tang, Internalization of exogenously added memapsin 2 (beta-secretase) ectodomain by cells is mediated by amyloid precursor protein, J. Biol. Chem. 279 (2004) 37886–37894.
[12] J.T. Huse, D.S. Pijak, G.J. Leslie, V.M. Lee, R.W. Doms, Maturation and endosomal targeting of beta-site amyloid precursor protein-cleaving enzyme. The Alzheimer's disease beta-secretase, J. Biol. Chem. 275 (2000) 33729–33737.
[13] E.H. Koo, S.L. Squazzo, Evidence that production and release of amyloid beta-protein involves the endocytic pathway, J. Biol. Chem. 269 (1994) 17386–17389.
[14] S.S. Sisodia, Beta-amyloid precursor protein cleavage by a membrane-bound protease, Proc. Natl. Acad. Sci. U. S. A. 89 (1992) 6075–6079.
[15] X. Lin, G. Koelsch, S. Wu, D. Downs, A. Dashti, J. Tang, Human aspartic protease memapsin 2 cleaves the beta-secretase site of beta-amyloid precursor protein, Proc. Natl. Acad. Sci. U. S. A. 97 (2000) 1456–1460.
[16] D.J. Owen, B.M. Collins, Vesicle transport: a new player in APP trafficking, Curr. Biol. 20 (2010) R413–R415.
[17] G. Thinakaran, E.H. Koo, Amyloid precursor protein trafficking, processing, and function, J. Biol. Chem. 283 (2008) 29615–29619.
[18] T. Suzuki, T. Nakaya, Regulation of amyloid beta-protein precursor by phosphorylation and protein interactions, J. Biol. Chem. 283 (2008) 29633–29637.
[19] C. Kaether, H.H. Gerdes, Visualization of protein transport along the secretory pathway using green fluorescent protein, FEBS Lett. 369 (1995) 267–271.
[20] Y. Qi, J.K.T. Wang, M. McMillian, D.M. Chikaraishi, Characterization of a CNS cell line, CAD, in which morphological differentiation is initiated by serum deprivation, J. Neurosci. 17 (4) (1997) 1217–1225.
[21] J. Tang, P. Sepulveda, J. Marciniszyn Jr., K.C. Chen, W.Y. Huang, N. Tao, D. Liu, J.P. Lanier, Amino-acid sequence of porcine pepsin, Proc. Natl. Acad. Sci. U. S. A. 70 (1973) 3437–3439.
[22] R.T. Turner III, L. Hong, G. Koelsch, A.K. Ghosh, J. Tang, Structural locations and functional roles of new subsites S5, S6, and S7 in memapsin 2 (beta-secretase), Biochemistry 44 (2005) 105–112.
[23] A.K. Ghosh, N. Kumaragurubaran, L. Hong, S. Kulkarni, X. Xu, H.B. Miller, D.S. Reddy, V. Weerasena, R. Turner, W. Chang, G. Koelsch, J. Tang, Potent memapsin 2 (beta-secretase) inhibitors: design, synthesis, protein-ligand X-ray structure, and in vivo evaluation, Bioorg. Med. Chem. Lett. 18 (2008) 1031–1036.
[24] R.M. Carey, B.A. Balcz, I. Lopez-Coviella, B.E. Slack, Inhibition of dynamin-dependent endocytosis increases shedding of the amyloid precursor protein ectodomain and reduces generation of amyloid beta protein, BMC Cell Biol. 6 (2005) 30.
[25] K. Offe, S.E. Dodson, J.T. Shoemaker, J.J. Fritz, M. Gearing, A.I. Levey, J.J. Lah, The lipoprotein receptor LR11 regulates amyloid beta production and amyloid precursor protein traffic in endosomal compartments, J. Neurosci. 26 (2006) 1596–1603.
[26] C.A. von Arnim, R. Spoelgen, I.D. Peltan, M. Deng, S. Courchesne, M. Koker, T. Matsui, H. Kowa, S.F. Lichtenthaler, M.C. Irizarry, B.T. Hyman, GGA1 acts as a spatial switch altering amyloid precursor protein trafficking and processing, J. Neurosci. 26 (2006) 9913–9922.
[27] S.I. Vieira Rebelo, E.F. da Cruz E Silva, O.A. da Cruz E Silva, Monitoring “De Novo” APP synthesis by taking advantage of the reversible effect of cycloheximide, Am. J. Alzheimer Dis. Other Demen. 23 (2008) 602–608.